Gas geochemistry of geothermal fluids from the Hatchobaru geothermal field, Japan

Ishibashi, Jun-ichiro ; Yamashita, Kei ; Kitamura, Keigo ; Fujimitsu, Yasuhiro ; Oshima, Syogo ; Kiyota, Yumi

(Citation)
Geothermics,102:102379

(Issue Date)
2022-06

(Resource Type)
journal article

(Version)
Accepted Manuscript

Gas geochemistry of geothermal fluids from the Hatchobaru geothermal field, Japan

Jun-ichiro Ishibashi [a, b, *], Kei Yamashita [a], Keigo Kitamura [c], Yasuhiro Fujimitsu [c], Syogo Oshima [d], Yumi Kiyota [d]

[a] Department of Earth and Planetary Sciences, Graduate School of Science, Kyushu University, Fukuoka, Japan

[b] Kobe University, Ocean-bottom Exploration Center, Kobe, Hyogo, Japan

[c] Department of Earth Resources Engineering, Faculty of Engineering, Kyushu University, Fukuoka, Japan

[d] Geothermal Department, West Japan Engineering Consultants, Inc., Fukuoka, Japan

*Corresponding author:
Ocean-bottom exploration center,
Kobe University
5-1-1 Fumake-minamimachi, Higashinada,
Kobe, Hyogo, 658-0022, Japan
Tel: +81 78 431 4639, Fax: +81 78 431 4620
E-mail address: ishibashi@port.kobe-u.ac.jp

Abstract

We analyzed the chemical and isotopic composition of the geothermal fluids from the Hatchobaru geothermal field in the Kyushu Island, Japan. Fluid chemistry showed similarity with that reported in earlier studies. Chemical geothermometry provided an estimated reservoir temperature of 250–300 °C. Helium and carbon isotopic ratios of the steam is likely to reflect the signature of the magmatic heat source. The apparent equilibrium temperature for carbon isotope exchange between CO_2 and CH_4 was 375–430 °C. The sulfur isotope data were in accordance with the idea that an acidic Cl-SO_4-type fluid was modified from a neutral Cl-type fluid.

Keywords

Estimated reservoir temperature

Magmatic volatiles

Carbon isotope exchange geothermometry

1. Introduction

Geochemical study of geothermal fluids is a useful technique for geothermal exploration. Chemical geothermometry is a conventional tool to estimate the temperature in the reservoir. It is based on the assumption that chemical interactions between the fluid and minerals of the surrounding rocks attained or at least were close to equilibrium. Moreover, the isotopic composition of specific species can provide information on their source. Geochemical data often support a model based on a geophysical survey, because they directly reflect the properties of the materials dissolved in the ascending fluid. Among them, gas species are considered to be mainly derived from the heat source magma, and can provide insights into the deeper region of the crust than from the fluid reservoir.

The Hatchobaru geothermal field is located in the central part of Kyushu Island and is one of the largest geothermal power plants in Japan. Geochemical studies have been conducted since the early stage of geothermal exploration in the 1960s (e.g., Hayashida and Ezima, 1970). Previous studies revealed two types of geothermal fluids: a neutral Cl-type fluid from the main reservoir and a Cl-SO_4-type fluid mainly recognized in the peripheral region (e.g., Shimada et al., 1985). Recent geochemical studies have focused on the acidic Cl-SO_4-type fluid (Kiyota et al., 1996; Matsuda et al., 2000); however, the gas chemistry of geothermal fluids has rarely been reported.

We had an opportunity to obtain the geothermal fluid samples directly from the well heads of the Hatchobaru geothermal power plant, using a portable phase separator that can collect the vapor phase (steam) without loss as well as the liquid phase (hot water). In this paper, we report the results of the chemical (major elements and gas species) and isotopic (gas phase) composition of the geothermal fluid from the Hatchobaru field. We also discuss the geochemical signature of the deep region of the geothermal system from the obtained data.

2. Geological background

The Hatchobaru geothermal field is located on the northwestern flank of the Kuju Volcanoes in central Kyushu Island, Japan (Fig. 1). The surrounding area is characterized by a graben structure, where active fault systems are concentrated. The heat source of the Hatchobaru geothermal field has been associated with the late Quaternary volcanic activity of the Kuju Volcanoes. Volcanic activity began at about 200 ka, and the most recent eruption was a small ash fall in 1995–1996 (Kamata and Kobayashi, 1997). On the east of the Hatchobaru geothermal field is Mt. Kurodake, which is a lava dome that formed at 1.6 ka.

The Hatchobaru geothermal field is stratigraphically divided into four units: 1) Kuju volcanic rocks (Middle–Upper Pleistocene) consisting of hornblende-bearing andesite lava, 2) Hohi volcanic rocks (Lower Pleistocene) consisting of pyroxene-bearing andesite lava flows, 3) Usa group (Miocene)

consisting of altered andesitic lava flows and brecciated tuff, and 4) basement rocks (pre-Tertiary) composed of granitic and metamorphic rocks, in a descending order (Fujino and Yamasaki, 1985).

The Hatchobaru geothermal system is mainly controlled by a fracture network consisting of a NW-SE trending and perpendicular NE-SW trending faults (Fig.1). Previous studies have revealed that the main reservoir of geothermal fluid is located in the southeastern part of the geothermal field, and the fluid ascends towards the northwest along the fault system (e.g., Shimada et al., 1994). Based on this understanding, production wells are arranged at depths of 1000–2300 m to collect the fluids for the power plant.

3. Methods

Geothermal fluid samples were collected from four production wells in the Hatchobaru geothermal power plant. Sampling was conducted in October and November 2018. Steam (vapor phase) and hot water (liquid phase) samples were collected separately by introducing the geothermal fluid discharge from each well head into a portable phase separator.

The hot water samples were collected in a polypropylene bottle and filtered with a 0.45 μm membrane filter within one hour. The filtered samples were divided into two bottles, one of which was acidified by HCl for cation analysis and the other for anion analysis. Chemical analysis of the hot water samples was conducted at Kyushu University. Major anions (Cl and SO_4) were analyzed using an ion chromatograph (DX-100, Thermo Scientific Dionex) after adequate dilution. Alkalinity analysis by titration with 0.1 N HCl was conducted for the quantitative determination of HCO_3. Major cations (Na, Mg, K, and Ca) together with other dominant species (SiO_2 and B) were analyzed using an ICP-OES (inductively coupled plasma-atomic emission spectrometer) (Model 5100, Agilent Technology, Tokyo) after adequate dilution. The precision for major element analysis was approximately ±10 % based on repeated analysis of a standard material. The isotopic compositions of hydrogen and oxygen were determined using a mass spectrometer following the conventional method. The sulfur isotopic composition of SO_4 was determined using an elemental analyzer/ mass spectrometer (EA/IRMS) after precipitation of $BaSO_4$. The precision for the isotope measurement was estimated as ±1 ‰ for hydrogen, ±0.1 ‰ for oxygen, and ±0.2 ‰ for sulfur.

The steam samples were collected following the conventional alkali absorption protocol (Orsat method). After condensation of H_2O, the non-condensable gas was introduced into the Cd acetate solution to precipitate CdS, which was later used for the determination of H_2S content and sulfur isotope measurements. Further, the non-condensable gas was introduced into a KOH solution, and the CO_2 content was determined from the difference in volume for the alkali absorption stage. The residual component (R-gas) was transferred into an evacuated bottle and provided for analysis using a gas chromatograph with a TCD (thermal conductivity detector) to determine the composition of the minor

gas species (N_2, O_2, H_2, CH_4, Ar, and He). The helium isotopic composition and He/Ne ratio was determined by samples collected separately into specific bottles using a high resolution mass spectrometer after purification procedure. The carbon isotopic composition of CO_2 was determined using a mass spectrometer with double inlets after precipitation of $BaCO_3$ from the KOH solution. The carbon isotopic composition of CH_4 in the R-gas fraction was determined using a gas chromatograph/combustion/mass spectrometer (GC/C/IRMS). The sulfur isotopic composition of H_2S was determined using an elemental analyzer/ mass spectrometer (EA/IRMS) after conversion of the CdS into $BaSO_4$. The precision for gas species analysis was approximately ±5 %, with the exception of trace amounts. The precision for isotope measurement was ±0.2 ‰ for both carbon and sulfur.

4. Results and discussion

4.1. Fluid chemistry

Table 1 summarizes the analytical results of the hot water (liquid phase) samples, including pH (measured at room temperature), major element concentrations, and isotopic ratios. Table 1 also presents the hot water data of samples collected during 1980–1997 from a previous report (NEDO, 2000) for comparison. Hydrogen and oxygen isotopic ratios were calculated to represent the single-phase geothermal fluid in the reservoir. The estimated reservoir temperatures by quartz solubility (Fournier, 1977) and by the Na-K-Ca geothermometer (Fournier and Truesdell, 1973) are also listed.

Similar to previous studies (e.g., Shimada et al., 1985; Kiyota et al., 1996), two types of geothermal fluids were recognized in the Hatchobaru geothermal field, which could be clearly distinguished by the pH of the hot waters, even when measured at room temperature. The neutral Cl-type fluid had a pH of 6–9, whereas the acidic Cl-SO_4-type fluid had a pH of 3–4. The neutral Cl-type fluid was enriched exclusively in Cl, whereas the acidic Cl-SO_4-type fluid contained some amount of SO_4 (Fig. 2a). The cation compositions of the two types of geothermal fluids were distinguished from the Giggenbach diagram (Giggenbach, 1988). The composition of the neutral Cl-type fluid plotted in a region that was close to the chemical equilibrium within the reservoir, whereas the composition of the acidic Cl-SO_4-type fluid plotted in the region of partial equilibrium (Fig. 2b).

The hydrogen and oxygen isotopic compositions of the studied geothermal fluids are plotted in a δD-$\delta^{18}O$ diagram (Fig. 3). Fig. 3 also shows the data of river water from the adjacent area (Amita and Ohsawa, 2003) for comparison. Both types of the Hatchobaru geothermal fluids revealed isotopic compositions that had clearly shifted from those of meteoric water. However, the deviation was not as large as to overlap with the high-temperature fumaroles of the Kuju-Iwoyama Volcano (shaded ellipse in Fig. 3).

The chemical geothermometer based on quartz solubility (Fournier, 1977) for the four samples yielded reservoir temperatures in a range from 255–270 °C (Table 1). The estimated reservoir

159 temperature from the samples collected in 1980–1997 showed a wider range, but their average value
160 was in agreement with those from the 2018 samples. The reservoir temperature estimated by the Na-
161 K-Ca geothermometer (Fournier and Truesdell, 1973) showed a range from 260–300 °C, which was
162 in good agreement with the estimation by the quartz geothermometer. Yahara and Tokita (2010) had
163 demonstrated that the reservoir temperature of the Hatchobaru geothermal field has been stable for at
164 least a few decades.
165 These fluid chemistry signatures are attributed to a stable geothermal system. Actually, chemical
166 composition of the fluid from Well 2H-21 did now show significant change between 1996 and 2018.
167 Recharge of meteoric water would have been abundant, and the discharging geothermal fluid would
168 have continually experienced matured fluid-mineral interactions within the reservoir. The neutral Cl-
169 type fluid could be denoted as the primary geothermal fluid, whereas the acidic Cl-SO_4-type fluid
170 could be considered as the modified by an additional sulfur-rich component based on the results of
171 Giggenbach diagram . Previous studies proposed dominant fluid-mineral interactions with andesitic
172 volcanic rocks, which overlie the granitic-metamorphic basement, based on a B/Cl molar ratio of ~0.05,
173 and Sr isotopic ratios (Shimada et al., 1994).
174
175 4.2. Gas chemistry
176 Table 2 summarizes the analytical results of the steam (vapor phase) samples that include
177 chemical and isotopic compositions of the gas species. The gas species composition was calculated in
178 ppm volume, which is similar to the value of μmol/mol, from analytical results of the non-condensable
179 gas or R-gas samples. The isotopic compositions of carbon for CO_2 and CH_4, sulfur for H_2S, and
180 helium are also listed in Table 2.
181 Composition of the gas species showed the typical signature of a water-dominated geothermal
182 system. As shown in a H_2O-CO_2-H_2S ternary diagram, the amount of non-condensable gas was less
183 than a few percent, and was mainly CO_2 with minor H_2S (Fig. 4a). Shimada et al. (1985) had proposed
184 that the CO_2/H_2S ratio of a fluid is associated with its pH, where the samples showed a high CO_2/H_2S
185 ratio of ~15 for the neutral Cl-type fluid, whereas this ratio was lower (<10) for the acidic Cl-SO_4-
186 type fluid. However, such an association was not distinctly observed in the studied samples (Fig. 4a).
187 The relative composition of the trace gas species is illustrated in a N_2-Ar-He ternary diagram (Fig. 4b).
188 In the diagram, the Hatchobaru geothermal fluid data are plotted along a trend between the air-
189 saturated water and the magmatic component represented by the gas composition of the fumaroles of
190 the Kuju-Iwoyama Volcano (shaded ellipse in Fig. 4b).
191 Both the helium and carbon isotopic compositions of the geothermal fluids were similar to those
192 of the magmatic component. The geothermal fluids were characterized by an elevated helium isotopic
193 composition ($^3He/^4He$ = [7.1−8.7] $\times 10^{-6}$) with a substantially high He/Ne ratio (Fig. 5), which
194 overlapped with the reported values from the fumaroles of the Kuju-Iwoyama Volcano (Marty et al.,

1989). These ratios were interpreted to be because of mixing between the magmatic component ($^3He/^4He = 8.4\times10^{-6}$) and the air-saturated water (Fig. 5). The carbon isotopic composition of CO_2 was in the range of $\delta^{13}C(CO_2) = -6.8$ to -4.4 ‰, which was consistent with the reported value of $\delta^{13}C(CO_2) = -8.0$ ‰ from the fumaroles of the Kuju-Iwoyama Volcano (Saito et al., 2002).

The geochemical signatures of the gas species suggest that the Hatchobaru geothermal system was affected by the subjacent magma with the contribution of magmatic volatiles (Hedenquist et al., 2018), although this contribution was not evident in the δD-$\delta^{18}O$ diagram (Fig. 3), where the observed shift was attributed to the influence of hot water that was injected into the adjacent subsurface through the reinjection wells (NEDO, 2000). The helium content of the gases showed a significant magmatic contribution (Fig. 4), and the elevated $^3He/^4He$ ratio was comparable to the highest range recognized among hot springs in the Kyushu Island which was attributed to the magma ascension into a relatively shallow depth (Horiguchi and Matsuda, 2013). Notably, no significant difference between the neutral Cl-type fluid and acidic Cl-SO_4-type fluid was recognized in the helium and carbon isotopic compositions of the studied samples, except for the sample from the H-33 well ($\delta^{13}C(CO_2) = -4.4$ ‰). The narrow range of isotopic ratios suggest limited opportunity for crustal contamination through the process of the expulsion of gas species from the heat source magma, involved into the geothermal fluid circulation, and transported to the surface as dissolved species.

4.3. Carbon and sulfur isotope systematics

The carbon and sulfur isotopic compositions were determined for the paired gas species. The isotopic data could provide temperature information based on isotope fractionation, when the paired species undergo significant mutual interactions in the deep region. A geothermometer based on carbon isotope fractionation between CO_2 and CH_4 has been applied to several geothermal fields, assuming that both species interact during the ascension of magmatic volatiles and/or in the fluid reservoir (e.g., Fiebig et al., 2004). This geothermometer is widely used as a carbon isotope measurement of trace amounts of CH_4 has become easier due to the progress in analytical instruments. However, the validity of this geothermometer is still questionable. Some recent studies argued a sluggish isotope exchange rate in natural systems due to a lack of efficient catalysts (e.g., McCollom, 2013). Others have demonstrated an unpreventable contribution of thermal degradation of organic matter in a geothermal system (e.g., Fiebig et al., 2019). Although the results must be interpreted with caution, discussion about the carbon isotopic composition of CH_4 in the context of a geothermometer could provide useful information about the deeper regions of the geothermal system.

The carbon isotopic data of CO_2 and CH_4 from the Hatchobaru geothermal fluid are plotted in Fig. 6, along with the apparent equilibrium temperatures (AETs) for carbon isotope exchange (Horita, 2001). The carbon isotope ratio of CH_4 showed a narrow range ($\delta^{13}C(CH_4) = -27.2$ to -23.5 ‰). The plots in Fig. 6 are aligned with the line parallel to the apparent equilibrium, even though one acidic

fluid sample (H-33 well) was scattered. The AET calculated from the isotope deviations of the four 2018 samples ranged from 375 to 430 °C (Table 2), which is distinctly higher than the estimated reservoir temperature of approximately 250–300 °C by chemical geothermometers. The carbon isotope systematics could be explained by interactions between CO_2 and CH_4 in a deeper region beneath the fluid reservoir. Such deep interaction zone is in accordance with a recent numerical model for the Hatchobaru geothermal system, where fluid supply was projected to occur from a deeper reservoir within the basement (Momita et al., 2000).

The sulfur isotope data for H_2S and SO_4 from the Hatchobaru fluid are plotted in Fig. 7. Although sulfur isotope deviations are not often used in geothermometry, AETs for sulfur isotope exchange (Ohmoto and Lasaga, 1982) were superimposed in Fig. 7. Notably, the neutral Cl-type fluid and acidic Cl-SO_4-type fluid showed similar sulfur isotope ratios of H_2S ($\delta^{34}S(H_2S)$ = −3.8 to −0.5 ‰), which overlapped with the magmatic value. For the Cl-type fluid, the apparent equilibrium temperature calculated from the isotope deviations was 265–320 °C, which was comparable to the estimated reservoir temperature of approximately 250–300 °C. These results could be explained by the presence of both H_2S and SO_4 during the process where the magmatic volatiles are involved into the fluid reservoir, and might be the result of a disproportional reaction. The acidic Cl-SO_4-type fluid showed not only a high SO_4 concentration but also ^{34}S-rich sulfur isotope ratio ($\delta^{34}S(SO_4)$ = +23.2 to +23.4 ‰) compared with that of the neutral Cl-type fluid ($\delta^{34}S(SO_4)$ = +9.0 to +20.0 ‰). This sulfur isotope systematics would be in accordance with the idea that contribution of an additional sulfur-rich component such as low-temperature fluids in the shallow level is an important factor for generation of the acid Cl-SO_4 type fluid (Matsuda et al., 2000).

5. Summary

We analyzed the liquid and vapor phases of the geothermal fluids obtained directly from the well heads of the Hatchobaru geothermal power plant. We conclude the following inferences from the fluid and gas chemistry of the studied samples from the Hatchobaru geothermal system:

(1) The major element composition and estimated reservoir temperature by conventional geothermometers showed little change over the past few decades. This suggests the stability of the geothermal system where fluid-mineral interactions sufficiently matured close to the chemical equilibrium within the reservoir.

(2) The helium and carbon (and possibly sulfur) isotopic compositions as well as gas compositions were similar to the reported values from the fumaroles of the nascent Kuju-Iwoyama Volcano. The gas chemistry strongly suggested that the geothermal system was substantially affected by the contribution of magmatic volatiles from the subjacent heat source.

(3) Carbon isotope systematics yielded an apparent equilibrium temperature of 375–430 °C, which is

distinctly higher than the estimated reservoir temperature. This result could be interpreted as reflecting the interaction between CO_2 and CH_4 in the deep region beneath the reservoir.

(4) Sulfur isotope systematics revealed different signatures between the neutral Cl-type fluid and acidic Cl-SO_4-type fluid. This difference is in accordance with the idea that the latter was modified by the contribution of an additional sulfur-rich component.

Acknowledgements

We appreciate cooperation of the Kyushu Electric Power Co., Inc. in sampling and permitting to publish the dataset. We express our special thanks to Kyuden Sangyo Co., Inc. for their sampling operation and analysis of gas species. We thank anonymous reviewers for constructive comments that helped improve the manuscript.

Funding

This study was conducted with support from the “Potential survey and estimation of power generation of supercritical geothermal resources in East Japan and Kyushu, Japan (FY2018-2020)” project that was funded by the New energy and industrial technology development organization (NEDO).

283 References

284 Amita, K., Ohsawa, S., 2003. Mixing process of air and underground water into magmatic gas
285 discharged from Kuju-Iwoyama fumarolic area of Kuju Volcano, Central Kyushu, Japan. Journal
286 of the Geothermal Research Society of Japan, 25, 245-265 (in Japanese with English abstract).
287 Fiebig, J., Chiodini, G., Caliro, S., Rizzo, A., Spangenberg, J., Hunziker, J.C., 2004. Chemical and
288 isotope equilibrium between CO_2 and CH_4 in fumarolic gas discharges: Generation of CH_4 in arc
289 magmatic-hydrothermal systems. Geochimica et Cosmochimica Acta, 68, 2221-2334.
290 Fiebig, J., Stefánsson, A., Ricci, A., Tassi, F., Viveiros, F., Silva, S., Lopez, T.M., Schreiber, C.,
291 Hofmann, S., Mountain, B.W., 2019. Abiogenesis not required to explain the origin of volcanic-
292 hydrothermal hydrocarbons. Geochemical Perspectives Letters, 11, 23-27.
293 Fournier, R.O., 1977. Chemical geothermometers and mixing models for geothermal systems.
294 Geothermics, 5, 41-50.
295 Fournier, R.O., Truesdell, A.H., 1973. An empirical Na-K-Ca geothermometer for natural waters.
296 Geochimica et Cosmochimica Acta, 37, 1255-1275.
297 Fujino, T., Yamasaki, T., 1985. Geologic and geothermal structure of the Hatchobaru field, Central
298 Kyushu, Japan. Geothermal resource council Bulletin 14, 11-15.
299 Giggenbach, W.F., 1988. Geothermal solute equilibria: Derivation of Na-K-Mg-Ca geoindicators.
300 Geochimica et Cosmochimica Acta, 52, 2749-2765.
301 Hayashida, T., Ezima, Y., 1970. Development of Otake geothermal field. Geothermics, 2, 208-220.
302 Hedenquist, J.W., Taguchi, S., Shinohara, H., 2018. Features of large magmatic-hydrothermal
303 systems in Japan: Characteristics similar to the tops of porphyry copper deposits. Resource
304 Geology, 68, 164-180.
305 Horiguchi, K., Matsuda, J., 2013. Geographical distribution of $^3He/^4He$ ratios in north Kyushu,
306 Japan: Geophysical implications for the occurrence of mantle-derived fluids at deep crustal levels.
307 Chemical Geology, 340, 13-20.
308 Horita, J., 2001. Carbon isotope exchange in the system CO_2-CH_4 at elevated temperatures.
309 Geochimica et Cosmochimica Acta, 65, 1907-1919.
310 Kamata, H., Kobayashi, T., 1997. The eruptive rate and history of Kuju Volcano in Japan during the
311 past 15,000 years. Journal of Volcanology and Geothermal Research, 76, 163-171.
312 Kiyota, Y., Matsuda, K., Shimada, K., 1996. Characterization of acid water in the Otake-Hatchobaru
313 geothermal field. Proceedings of the 17th annual PNOC-EDC geothermal conference, Manila,
314 Philippines. Energy Development Corporation, Manila, 131-135.
315 Marty, B., Jambon, A., Sano, Y., 1989. Helium isotopes and CO_2 in volcanic gases of Japan.
316 Chemical Geology, 76, 25-40.
317 Matsuda, K., Shimada, K., Kiyota, Y., 2000. Development of study methods for clarifying formation
318 mechanism and distribution of acid geothermal-fluid -Case studies of geothermal areas in Kyushu-

Japan. Proceedings of the world geothermal congress 2000, Kyushu Tohoku, Japan, 1425-1430.
McCollom, T.M., 2013. Laboratory simulations of abiotic hydrocarbon formation in Earth's deep subsurface. Reviews in Mineralogy and Geochemistry, 75, 467-494.
Momita, M., Tokita, H., Matsuda, K., Takagi, H., Soeda, Y., Tosha, T., Koide, K., 2000. Deep geothermal structure and the hydrothermal system in the Otake Hatchobaru geothermal field, Japan. Proceedings of the 22nd New Zealand geothermal workshop, Auckland, New Zealand, 257-262.
NEDO, 2000. Report of Deep-Seated Geothermal Resources Survey Project. New Energy Development Organization (NEDO), Kawasaki. (in Japanese).
Ohmoto, H., Lasaga, A.C., 1982. Kinetics of reactions between aqueous sulfates and sulfides in hydrothermal systems. Geochimica et Cosmochimica Acta, 46, 1727-1745.
Saito, G., Shinohara, H., Kazahaya, K., 2002. Successive sampling of fumarolic gases at Satsuma-Iwojima and Kuju volcanoes, southwest Japan: Evaluation of short-term variations and precision of the gas sampling and analytical techniques. Geochemical Journal, 36, 1-20.
Shimada, K., Fujino, T., Koga, A., Hirowatari, K., 1985. Acid hot water discharging from geothermal wells in the Hatchobaru geothermal field. Chinetsu (Journal of the Japan Geothermal Energy Association), 22, 276-292 (in Japanese with English abstract).
Shimada, K., Tagomori, K., Fujino, T., Kitakoga, I., 1994. Deep geothermal structure and targets of future development in the Hatchobaru geothermal field, Chinetsu (Journal of the Japan Geothermal Energy Association), 31, 301-319 (in Japanese with English abstract).
Yahara, T., Tokita, H., 2010. Sustainability of the Hatchobaru geothermal field, Japan. Geothermics, 39, 382-390.

Figure Captions:

Fig. 1: Topographic map of the area surrounding the Hatchobaru geothermal power plant (GPP). The locality is shown as a star mark in the insertion map. Active faults and inferred faults are illustrated as solid and dashed lines with bars. The peaks of Quaternary volcanoes are shown as triangles. The shaded ellipse shows the locality of the fumaroles of the Kuju-Iwoyama Volcano from where fumarole samples were collected in the previous studies (Amita and Ohsawa, 2003; Saito et al., 2002; Marty et al., 1989).

Fig. 2: Major element compositions of the Hatchobaru geothermal fluids. (a) anion composition in the trilinear diagram and (b) cation composition plotted in the Giggenbach diagram. Closed circles represent the acidic Cl-SO_4-type fluid and open squares represent the neutral Cl-type fluid (smaller symbols indicate data of geothermal fluids collected during 1980–1998 from NEDO (2000)).

Fig. 3: Hydrogen and oxygen isotopic compositions of the Hatchobaru geothermal fluids. Close circles and open square symbols are same as for Figure 2. Cross marks indicate isotopic compositions of cold springs and river waters in the adjacent area, and the shaded ellipse shows the data range of high temperature fumaroles from the Kuju-Iwoyama Volcano (Data Sources: Amita and Ohsawa, 2003).

Fig. 4: Gas species composition of the Hatchobaru geothermal fluids. (a) relationship between H_2O, CO_2 and H_2S, and (b) relationship between N_2, Ar, and He. Close circles and open square symbols are same as for Figure 2 (smaller symbols indicate data of geothermal fluids collected during 1992–1998 from NEDO (2000)). Cross marks in (b) indicate the value of the air-saturated water. The range of high temperature fumaroles from the Kuju-Iwoyama Volcano is shown in arrow marks in (a) and as shaded elipse in (b) (Data Sources: Amita and Ohsawa, 2003).

Fig. 5: Relationship between $^3He/^4He$ and He/Ne for the Hatchobaru geothermal fluids. Note that both axes are shown in a log scale. Close circles and open square symbols are same as for Figure 2. Mixing curve between the air-saturated water (cross mark) and the endmember that has $^3He/^4He = 8.4 \times 10^{-6}$ is illustrated. A close triangle indicates data of high temperature fumaroles from the Kuju-Iwoyama Volcano (Data Sources: Marty et al., 1989).

Fig. 6: Relationship between $\delta^{13}C(CH_4)$ and $\delta^{13}C(CO_2)$ for the Hatchobaru geothermal fluids. Close circles and open square symbols are same as for Figure 2. Dashed lines indicate apparent equilibrium temperature for carbon isotope exchange calculated from Horita et al. (2001).

Fig. 7: Relationship between $\delta^{34}S(H_2S)$ and $\delta^{34}S(SO_4)$ for the Hatchobaru geothermal fluids. Close circles and open square symbols are same as for Figure 2. Dashed lines indicate apparent equilibrium temperature for carbon isotope exchange calculated from Ohmoto and Lasaga (1982).

Table 1 Chemical and isotopic compositions of hot waters collected from the Hatchobaru power station

Well ID	Sampling date	pH	Na (mg/L)	K (mg/L)	Mg (mg/L)	Ca (mg/L)	Cl (mg/L)	SO_4 (mg/L)	HCO_3 (mg/L)	B (mg/L)	SiO_2 (mg/L)	$\delta D^{\#}$ (‰)	$\delta^{18}O^{\#}$ (‰)	$\delta^{34}S(SO_4)$ (‰)	t_{qtz} (°C)	$t_{Na\text{-}K\text{-}Ca}$ (°C)
2H-21	2018/10/18	7.7	1630	286	<d.l.	6.70	2620	80.0	33.6	34.3	784	-53	-6.0	+18.4	260	280
H-32	2018/11/20	7.2	1630	251	<d.l.	12.3	2450	170	23.1	34.0	733	-56	-6.5	+18.3	255	261
H-33	2018/11/21	3.1	1050	179	2.8	6.89	1390	398	<d.l.	23.0	797	-59	-6.1	+23.4	261	266
H-34	2018/11/22	8.3	1190	258	<d.l.	3.61	1790	80.0	82.6	26.9	879	-58	-6.6	+19.2	269	297
H-4*	1981/2/5	7.9	1995	226	2.0	83.8	3505	190	8.0	43.2	510	-56.6	-4.7	+20.0	227	222
2H-21*	1996/3/1	6.4	1590	328	0.1	14.4	2750	85.8	15.0	39.2	1088	-53.9	-6.7	+16.2	285	282
H-28*	1995/10/17	3.4	1293	260	15.0	16.2	1830	747	<d.l.	23.9	729	-59.5	-7.2	+23.2	249	273
H-29*	1997/9/11	3.2	1090	228	12.7	11.6	1530	739	<d.l.	20.5	637	-56.3	-7.0	+23.2	241	276
HT-3*	1980/8/25	3.3	1360	211	5.7	6.69	2230	349	<d.l.	28.9	691	n.d.	n.d.	n.d.	250	265
HT-5-1*	1982/4/20	8.6	1330	245	0.16	9.3	2240	71.0	227	32.5	1050	-55.8	-6.6	+ 9.0	281	284
2HD-1*	1998/6/25	8.5	1070	234	0.01	5.59	1540	26.9	97.7	32.3	1120	-59.6	-5.5	+16.5	288	289

<d.l.= below the detection limit, n.d.= no data

Hydrogen and oxygen isotope composition was corrected to estimate isotope compositions of the reservoir

* Data of the samples collected during 1980-1997 are cited from NEDO (2000).

Table 2 Chemical and isotopic composition of steams collected from the Hatchobaru power station

Well ID	Sampling date	H_2O (vol%)	CO_2 (ppm)	H_2S (ppm)	N_2 (ppm)	O_2 (ppm)	H_2 (ppm)	CH_4 (ppm)	Ar (ppm)	He (ppm)	$\delta^{13}C(CO_2)$ (‰)	$\delta^{13}C(CH_4)$ (‰)	$\delta^{34}S(H_2S)$ (‰)	$^3He/^4He$ ($\times10^{-6}$)	$^4He/^{20}Ne$
2H-21	2018/10/18	99.9	650	117	17.9	0.7	2.2	1.0	0.3	0.006	-6.6	-25.3	-0.5	8.66±0.08	18.3
H-32	2018/11/20	99.9	624	146	22.9	1.7	4.1	0.5	0.3	0.003	-6.7	-27.2	-3.7	7.14±0.08	18.8
H-33	2018/11/21	99.2	7140	351	100	6.7	8.6	35.8	1.3	0.086	-4.4	-23.5	-2.4	8.14±0.09	54.1
H-34	2018/11/22	99.6	4010	202	54.6	1.4	5.7	18.9	0.8	0.038	-6.8	-24.5	-3.8	7.68±0.07	62.5

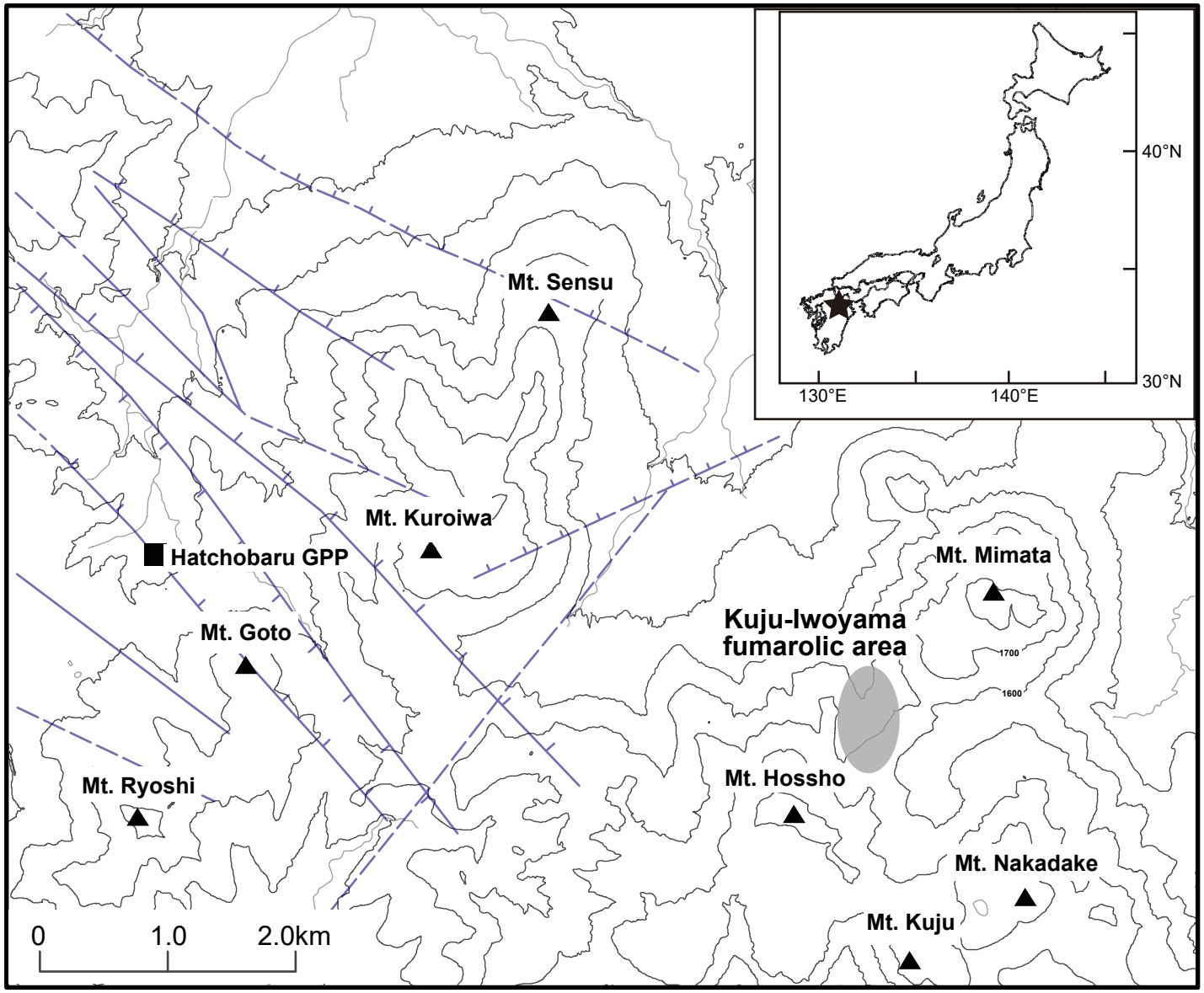

Fig. 1 (Ishibashi et al.)

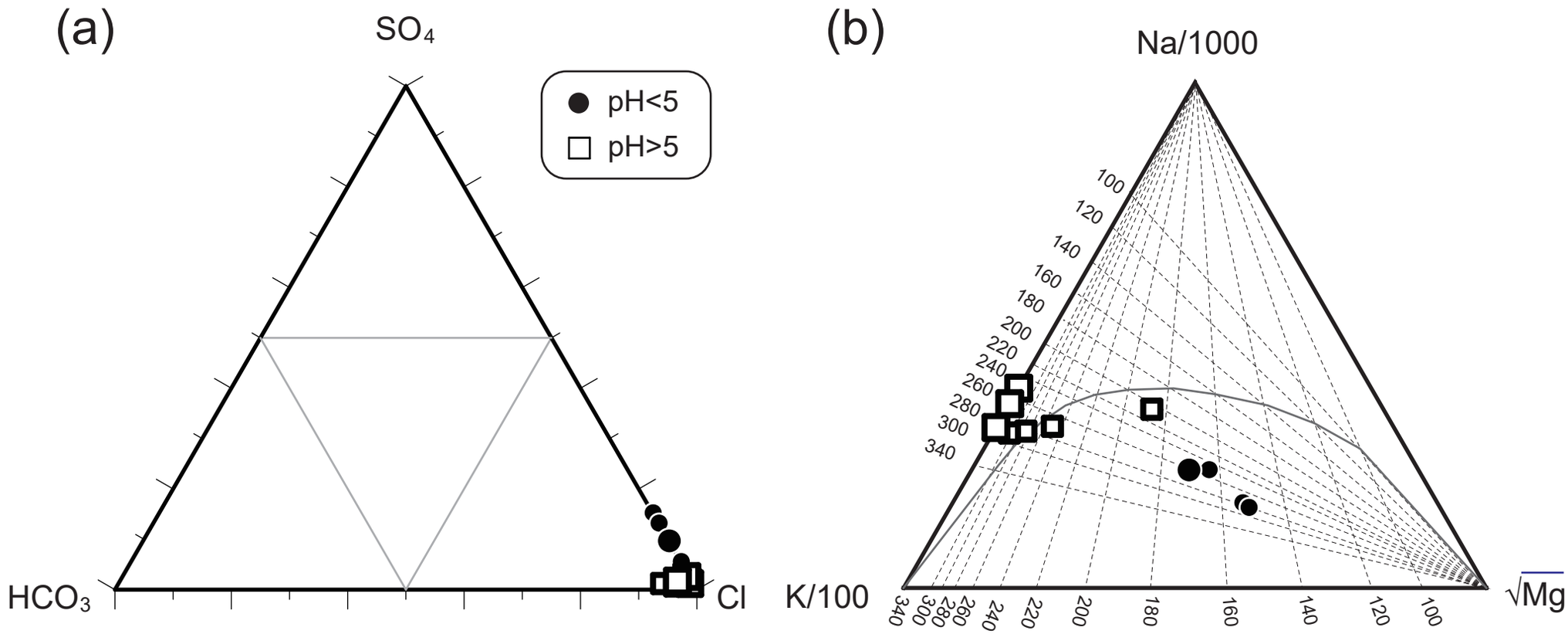

Fig. 2 (Ishibashi et al.)

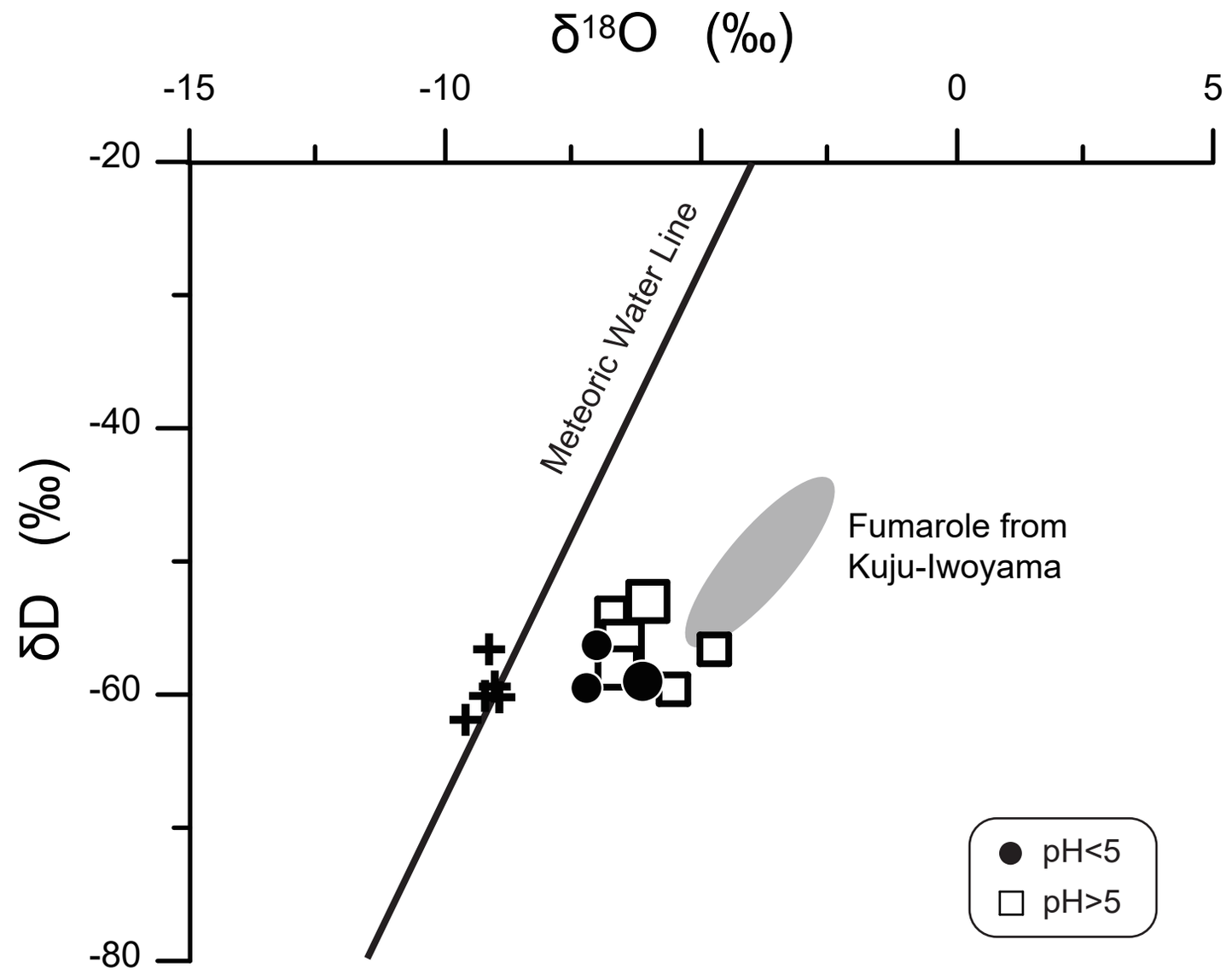

Fig. 3 (Ishibashi et al.)

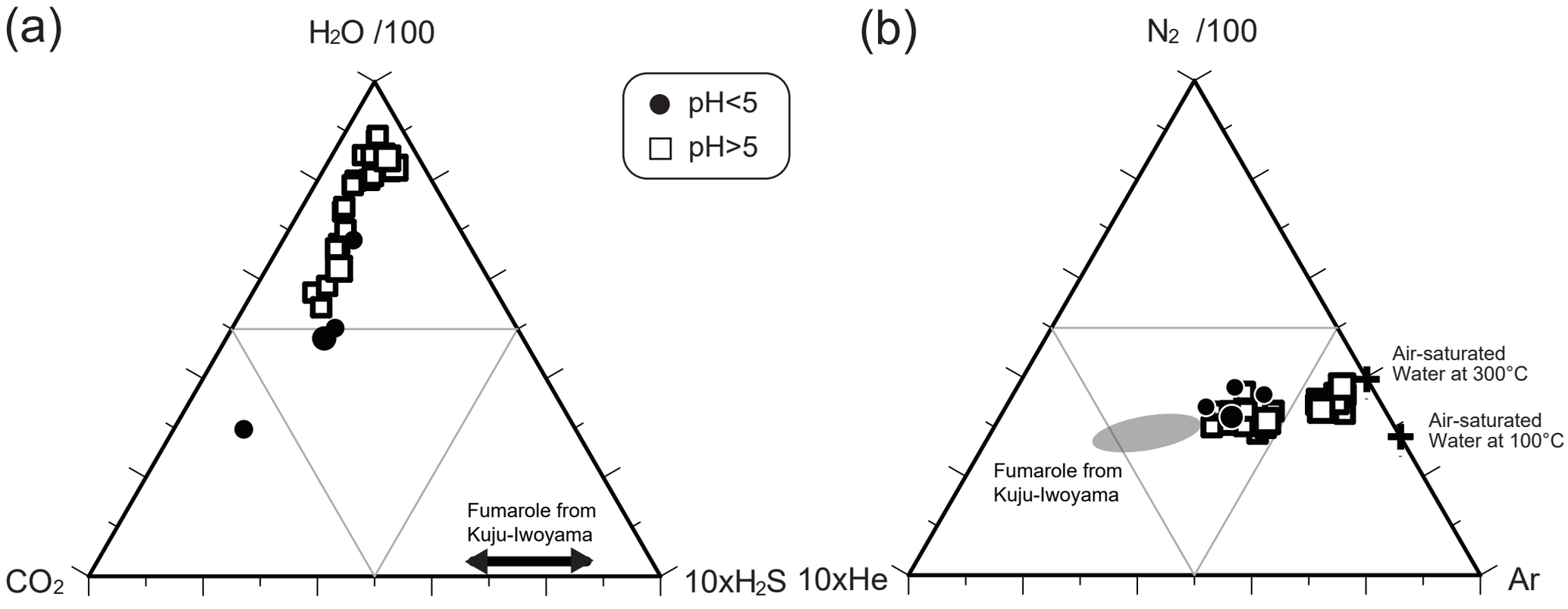

Fig. 4 (Ishibashi et al.)

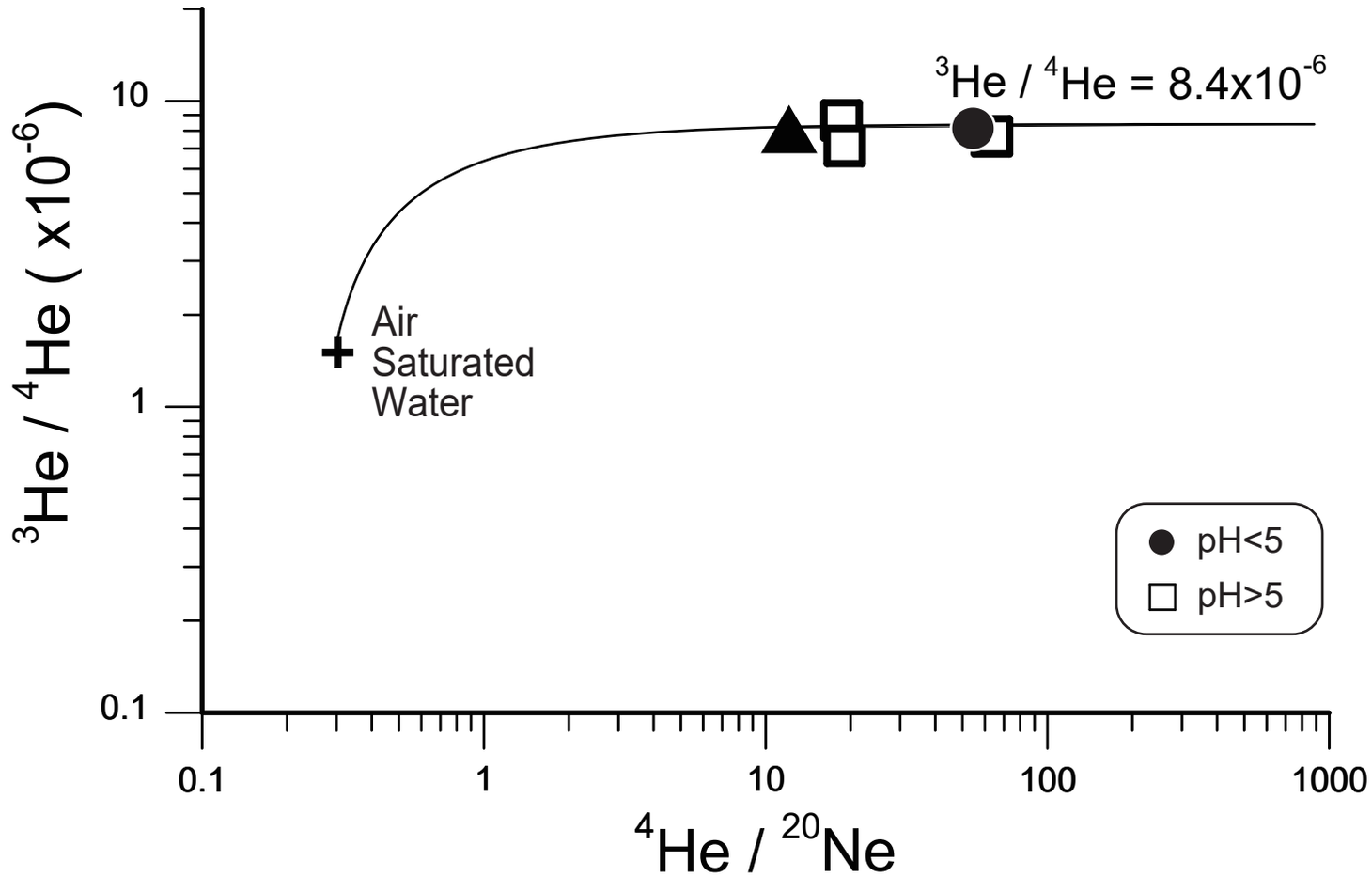

Fig. 5 (Ishibashi et al.)

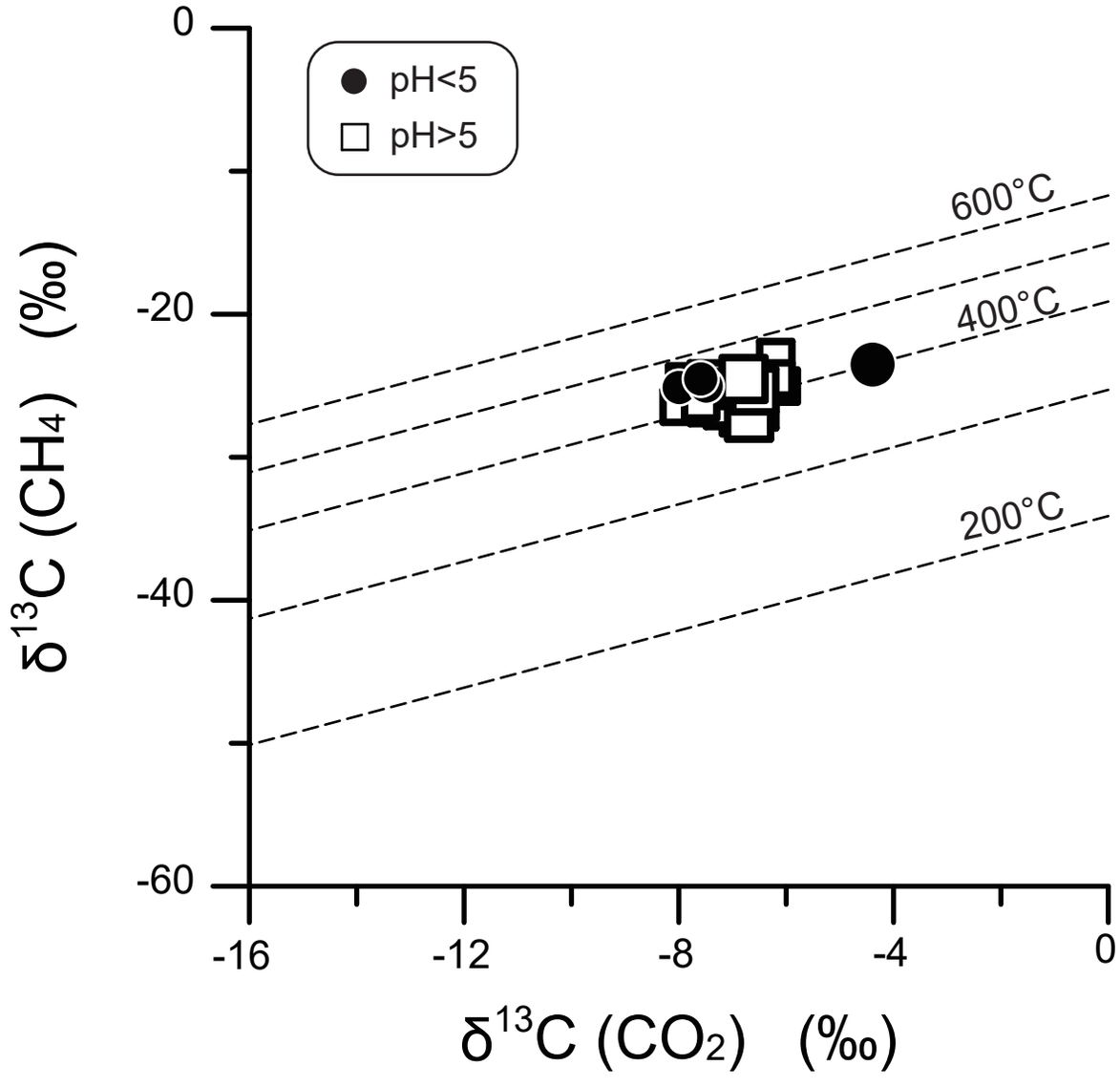

Fig. 6 (Ishibashi et al.)

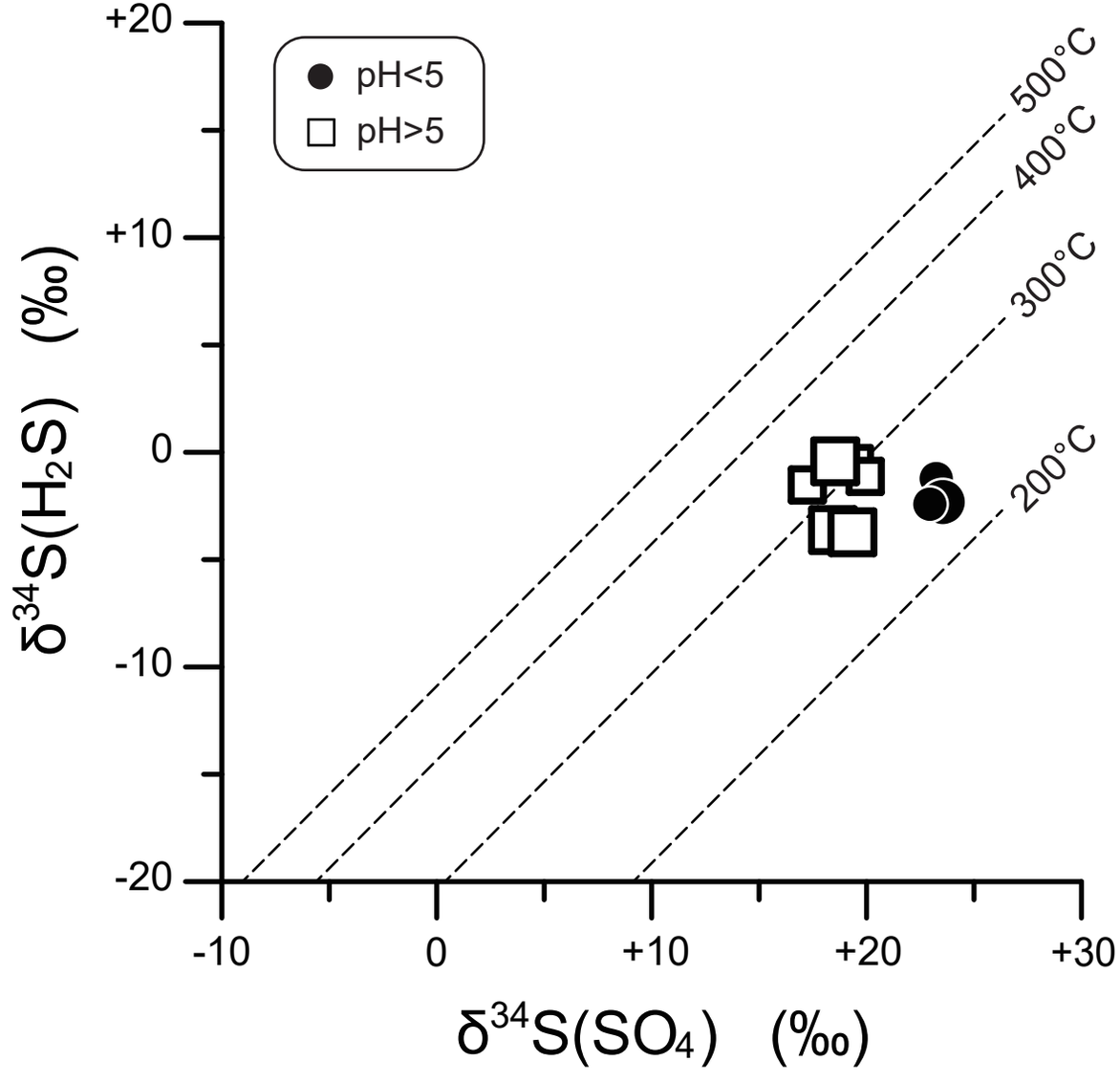

Fig. 7 (Ishibashi et al.)